International Journal of
Science and Engineering Investigations vol. 6, issue 61, February 2017
ISSN: 2251-8843

Modeling the Performance of Multi-Pass Solar Crop Dryer with Reversed Absorber

Vijay R. Khawale[1], Shashank Thakare[2]
[1]Mechanical Department, Asst. Professor, Dr. Babasaheb Ambedkar College of Engineering and Research, Nagpur, India
[2]Mechanical Department, Professor, Prof. Ram Meghe Institute of Technology and Research, Amravati, India
([1]vrk4671@rediffmail.com, [2]sbthakare2007@gmail.com)

Abstract- In the present communication, performance of a new designed multi-pass solar crop dryer with reversed absorber (MPRASCD) was investigated experimentally and were compared with those of a typical single glazing and multi-pass solar crop dryer (MPSCD). Energy equation was developed for all the elements of solar air heater to validate the performance of multi pass solar air heater with reversed absorber. The result of a multi pass solar crop dryer with reversed absorber when compared with a multi pass solar air heater and single glazing solar crop dryer with and without reflector shows a considerable improvement in the collector efficiency, drying efficiency and pick-up efficiency. For the same flow rate, the efficiency of the solar crop dryer with reversed absorber is found to be higher than the solar crop dryer without reversed absorber solar air heater by 4.23-10%. Moisture content of red chili was reduced from 79.1% (wb) to 9.1% (wb) in 22 h by using MPRASCD and it took 30 h in MPSCD. The values of the coefficient of determination (R^2), mean bias error (MBE) and root mean square error (RMSE) are used to find dependability and the quality of the fit. The Page's model is showed a better fit to drying red chili among Newton model and Hederson & Pabis model.

Keywords-*Energy Equation, Solar Air Heater, Multi Pass, Reversed Absorber, Efficiency*

I. INTRODUCTION

Solar drying has been verified to be an economical and useful option to traditional and mechanical drying systems, particularly in locations with good sunshine during the harvest season. Solar air collector is a main component of solar dryer. A solar air heater provides the high temperature air (40 - 65°C) to the dryer only during sunshine hours. For drying agricultural products various types of solar drying systems were used [1]. Lower thermal efficiency is the disadvantage of conventional solar air collectors. Collector efficiency can be increased by extending the heat transfer area by using finned absorber [2-7], corrugated surface [8], and porous media [9]. Fudholi et al. [2, 3 and 8] reported that when the volume flow rate of air was 6.8 m3/s then V groove collector was more efficient than conventional solar air heater. Further he reported that when the solar radiation was 420 W/m2 to 790 W/m2 and mass flow rate 0.04 kg/s to 0.08 kg/s then finned absorber were more efficient than conventional solar air heater i.e 2 to 8%. .Sopian et al. [9] noted that thermal efficiency of the double-pass solar air collector is about 60-70% with porous absorber. R. K. Goyal et al. [10] used a concept of reverse flat plate collector as a heating medium of air for the drying of agricultural products in a cabinet dryer. The reverse flat plate absorber was a non-concentrating collector which can collect solar heat at high temperature unlike conventional non concentrating collectors. The performance of this system was compared with that of conventional cabinet dryers. It was found that the reverse flat plate absorber dryer gives the better performance. Jain and jain (11) reported that a multi-tray crop dryer with inclined multi-pass air heater with in-built thermal storage were more efficient than conventional solar air heater. Jain [12] investigated a transient analytical model to study the new concept of a solar crop dryer having reversed absorber plate type collector and thermal storage with natural airflow and reported a high temperature of reversed absorber than inclined absorber.

II. MATERIALS AND M,ETHODS

A. Experimental set up

A schematic diagram of a proposed force circulation multi pass solar crop dryer with a reversed absorber plate is shown in Fig.1 It consists of the two glass cover of 4 mm thick, two black painted aluminum absorber plates and an aluminum foil covered reflector. A reflector like a part of polygonal form (pieces of five equal flat surfaces) is located under the flat plate absorber-II. The size of the collector is 1 m wide and 2 m long. The gap between the two glass cover-I & II and glass cover-II and absorber-I surface were maintained at 25 mm. The solar air heater is slanting to face south and tilted at 31°C angle from the horizontal plane to make best use of the solar energy incident on the solar collector. The air is to be heated when it flows between the two glass cover (I & II) and then enter into the gap formed by glass cover-II and absorber plate –I (25mm), finally it passes through the passage formed by absorber plate-I & II where it gains the thermal energy from absorber plate-I & II. Thus the temperature of air gets maximized in a solar air heater. The outlet air from solar air heater is used for chili drying.

The experimental setup mainly consists of a solar air heater, reflector, drying chamber, Exhaust fan with variable speed controller, Six pre calibrated RTD (pt100) temperature sensor with ±0.5 °C accuracy were fixed at different location of the solar dryer are connected to a digital temperature indicator (having 0.1°C resolution) through a rotary switch, Pyranometer (Range: 1999 W/m²) Accuracy : ±10 W/m², (Make- TENMARS Electronics Co., Ltd. Taiwan), Anemometer (Range: 20 m/s) Accuracy: ±0.01m/s, (Make- MECO instrument**),** Wet and Dry bulb Hygrometer (Make- OMSONS).The drying cabinet was made of insulated wooden walls of dimensions 1 m length, 1 m breadth and 1 m height.

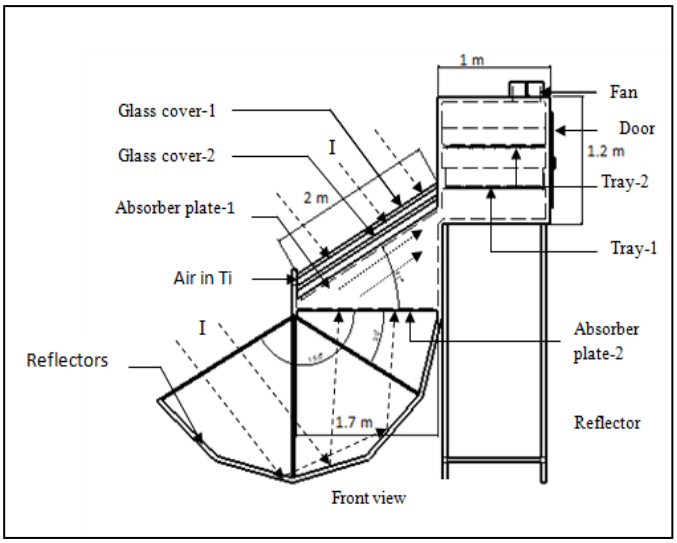

Figure 1. Schematic diagram of Multi pass solar crop dryer with reversed absorber (MPRASCD)

Exhaust fan with an air flow rate up to 300 m³/ h was provided at the top of drying cabinet. The fan used to maintain a constant flow rate (v=1m/s) in a solar air heater and drying chamber.

Experimental study was conducted from March 2 to March 19, 2016 in the natural wind. During this period, the weather condition was conventional, which made the conditions of experiments quite simple, experimental site is: 324.42m from mean sea level, India, Latitude 21.1458 North, Longitude 79.088 East.

III. THERMAL ANALYSIS

The solar radiation transmits from the glass covers and reflector which is absorbed by the absorber plate. The air flows in between the glass covers, above the absorber plate and below the absorber plate, where it is heated along the path. The energy balance equations on the various components of the system are written with the following assumptions:

i. The heat capacities of the insulation are negligible,

ii. There is no temperature gradient along the thickness of glass cover,

iii. The system is perfectly insulated and there is no air leakage,

iv. The heat flow is one dimensional and in a quasi-steady state condition,

v. All convection heat transfer coefficients in channels and flowing air are equal and constant,

vi. Thermal conductivity of absorber is constant,

vii. The useful heat gain to the air is uniform along the length of the collector [5, 7 and 13].

a) For first glass cover

$$I\alpha g1 Ag1 + hrg2g1\,(Tg2 - Tg1)\,Ag1 = hcg1f1\,(Tg1 - Tf1)\,Ag1 + hcg1a\,(Tg1 - Ta)\,Ag1 + hrg1sky\,(Tg1 - Tsky)\,Ag1 \quad (1)$$

Where Tsky = Ta-6 (whiller, 1967)

b) For second glass cover

$$I\tau g2\,\alpha g2 + hrp1g2\,(Tp1 - Tg2) + hcf1g2\,(Tf1 - Tg2) = hrg2g1\,(Tg2 - Tg1) + hcg2f2\,(Tg2 - Tf2) \quad (2)$$

c) For the absorber plate –I

$$I.\alpha p.\tau g1.\tau g2 = hrp1g2\,(Tp1 - Tg2) + hcp1f2\,(Tp1 - Tf2) + hrp1p2\,(Tp2 - Tp1 + hcp1f3\,(Tp1 - Tf3) \quad (3)$$

d) For absorber plate – II

$$Ieff.\alpha p = hrp1p2\,(Tp2 - Tp1) + hc.p2f3\,(Tp2 - Tf3) + hrp2a\,(Tp2 - Ta) + hcp2a\,(Tp2 - Ta) \quad (4)$$

Where, Ieff = (I.ρ′.Ar)/Ap effective solar radiation per unit area on the absorber plate – II

e) For air stream –I

$$hcg1f1\,(Tg1 - Tf1) = m.C.\Delta Tf1/WL + hcf1g2\,(Tf1 - Tg2) \quad (5)$$

f) For air stream – II

$$hcg2f2\,(Tg2 - Tf2) + hcp1f2\,(Tp1 - Tf2) = m.C.\Delta Tf2/WL \quad (6)$$

g) For air stream- III

$$hcp2f3\,(Tp2 - Tf3) + hcp1f3\,(Tp1 - Tf3) = m.C.\Delta Tf3/WL \quad (7)$$

The theoretical model assumed that, the temperatures of the wall surrounding the airflow are uniform, and the temperature of the airflow varies linearly along the collector.

For the collector mean air temperature is then equal to arithmetic mean.

$$Tf1 = \frac{(Tf1,0 + Ti)}{2} \quad (8)$$

$$Tf2 = \frac{(Tf2,0 + Tf1,0)}{2} \quad (9)$$

$$Tf3 = \frac{(Tf3,0 + Tf2,0)}{2} \quad (10)$$

In general, Eq. 1 to 7 above can be presented in a 7×7 matrix form.

$$[A][T] = [S] \quad (11)$$

Where

$$S1 = \alpha g1I + hcg1a\ Ta + hrg1Sky.Tsky \quad (13)$$

$$S2 = m.C / WL \quad (14)$$

$$S3 = \tau g2.\alpha g2.I \quad (15)$$

$$S4 = m.C /WL \quad (16)$$

$$S5 = \tau g1.\tau g2.\alpha p\ I \quad (17)$$

$$S6 = (m.C/WL)\ Tf2 \quad (18)$$

$$S7 = \alpha p.I.\rho'Ar + hrp2a.Ta + hcp2a.Ta \quad (19)$$

$$S8 = hcg1f1 + hrg2g1 + hrg1Sky + hcg1a \quad (20)$$

$$S9 = hcg1Tf1 + hcf1g2 + m.C /WL \quad (21)$$

$$S10 = hrp1g2 + hcf1g2 + hrg2g1 + hcg2f1 \quad (22)$$

$$S11 = hcg2f2 + hcp1f2 + m.C /WL \quad (23)$$

$$S12 = hrp1g2 + hcp1f2 + hrp1p2 + hcp1f3 \quad (24)$$

$$S13 = hcp2f3 + hcp1f3 + m.C /WL \quad (25)$$

$$S14 = hrp1p2 + hcp2f3 + hcp2a + hcp2a \quad (26)$$

The mean temperature vector may be determined with Excel by matrix inversion form

$$[T] = [A]^{-1}[S \quad (27)$$

A. Input parameters

Solar intensities on the different inclined surface of reflectors and 31°C tilted absorber were computed by using the method given by Lui and Jordan (1962)[14].

The effective solar intensity (Ieff.) available for the reversed absorber plate –II and solar intensity of inclined (β=31°) absorber plate-I are equal throughout the day [12].

The newly computed temperatures were compared with the experimentally observed values and then computed repeatedly until all consecutive mean temperatures differed by less than 1°C. In the present study, sufficient convergence for Tg1, Tg2, Tf1, Tf2, Tf3, Tp1, and Tp2 was achieved in four to six iterations. The major design parameters are as follows: L = 2 m, W = 1 m, H = 0.025 m, αp = 0.95, αg = 0.05, εp = 0.9, εg = 0.8, τg = 0.92, Ta = 25°C, Ti = 27°C and V = 1 m/s.

The efficiency of the solar collector is calculated from,

$$\text{Ƞc} = \frac{m.C\ (Tf-Ti)}{AI} \quad (28)$$

Where

Tf and Ti are outlet and inlet temperature of air

The physical properties of air are assumed to vary linearly with temperature (°C) by ONG [15];

Specific heat

$$C=1.0057+0.0000669(T-27) \quad (29)$$

Density

$$P=1.1774–0.00359(T-27) \quad (30)$$

Thermal conductivity

$$K=0.02624+0.0000758(T-27) \quad (31)$$

Viscosity

$$\mu=[1.983+0.00184(T-27)]10^{-5} \quad (32)$$

The heat transfer coefficient computed accordingly, Such as

$$hw=2.8+3. \quad (33)$$

Where hw is the convection heat transfer coefficient due to wind and V is the wind velocity.

$$hrgs = \frac{\sigma\ \varepsilon g(Tg+Ts)(Tg^2+Ts^2)(Tg-Ts)}{Tg-Ta} \quad (34)$$

Ts is the sky temperature, (Ts = Ta – 6)

$$Ut = \left(\frac{1}{hw+hrgs}\right)^{-1} \quad (35)$$

The convective heat transfer coefficients is calculated using following relations,

$$h = \frac{k}{de}Nu \quad (36)$$

Where Nu is Nusselt number and de is the equivalence diameter of the channel. For laminar flow region,

Nusselt number for (Re<2300) [15-17]:

$$Nu = 5.4 + \frac{0.00190[Re\ Pr\left(\frac{de}{L}\right)]^{1.71}}{1+0.00563[Re\ \Pr\left(\frac{de}{L}\right)]^{1.71}} \quad (37)$$

For transition flow region (2300 < Re < 6000)

$$Nu = 0.116(Re^{⅔} - 125)Pr^{⅓}[1 + \left(\frac{de}{L}\right)^{⅔}]\left(\frac{\mu}{\mu w}\right)^{0.14} \quad (38)$$

For turbulent flow region

$$Nu = 0.018\ Re^{0.8}\ Pr^{0.4} \quad (39)$$

$$Re = \frac{\rho v de}{\mu} \quad (40)$$

$$de = \frac{4\ W\ h}{2(W+h)} \quad (41)$$

A steady state form solution to determine the outlet temperature was obtained for energy balance equations. It solves the simultaneous equations for temperature at each element of a multi pass solar air collector with reversed absorber. A matrix inversion method was employed. For given sets of operating conditions the theoretical and experimental efficiency of a multi pass solar air collector with reversed absorber can be obtained.

IV. Mathematical Modeling of Drying Curves

For mathematical modeling the thin layer drying equations in Table 1 were tested to select the best model for describing the drying curve equation for red chili drying [9, 10-14, 15-17,]. Following equations were used to calculate the system performance and the drying characteristics of chili drying.

During experimentation the moisture content was calculated on wet basis and then converted to kg water per kg dry matter (db).

The moisture content on dry basis is the weight of moisture present in the chili per unit weight of dry matter in the chili and is expressed as [18]

Initial moisture content Mi= $\frac{Ws-Wd}{Wd}$ (42)

Final moisture content Mf = $\frac{Wwet-Wd}{Wd}$ (43)

ws = weight of sample at t=0 (kg)

wd = mass of dry matter (kg)

wwet = mass of wet matter after drying in a solar dryer

wt = weight of sample at any time 't' (kg)

The instantaneous moisture content (Mt) was calculated using the following expression at any given time on dry basis [19]

$Mt = \frac{(Wt-Wd)}{Wd}$ (44)

The change in weight of chili over a time during experimentation was used to calculate the moisture change in chili with respective time [19]. A drying rate constant 'k' was derived from the plot by fitting moisture ratio and time to a thin layer drying equation.

Moisture ratio $MR = \frac{Mt-Me}{Mi-Me} = e^{-kt}$ (45)

Where,

Me = Equilibrium moisture content

Mi = Initial moisture content

Since equilibrium moisture content was small as compared to initial and instantaneous moisture content for long period drying and continuous fluctuation of the relative humidity of the drying air during solar drying, the expression (6) can be express as [20],

Moisture ratio $MR = \frac{Mt}{Mi} = e^{-kt}$ (46)

Drying rate, drying efficiency and pick-up efficiency are the main characteristics to evaluate the performance of any solar drying systems [21]. The drying rate is proportional to the difference in moisture content in dried food product and the equilibrium moisture content [22], which is expressed as thin layer equation,

Drying rate dM/dt = -k (Mt–Me) (47)

Dryer thermal efficiency was calculated from the expression [18],

$\eta d = \frac{mw.Hg}{ma\ Cp(Td-Ti)}$ (48)

Where mw is the mass of water evaporated, hfg is the latent heat of evaporation of water, ma is the air mass flow rate in the dryer, cp is the specific heat of air, Td is the dryer air temperature and Ti is the air temperature at collector inlet which can be taken equal to ambient temperature.

The dryer pick-up efficiency was calculated from the expression [19],

$\eta p = \frac{Mw}{Ma\ \Delta t(Wde-Wdi)}$ (49)

Where mw is the mass of moisture evaporated in time Δt, ma is the mass flow rate of air, Wde is the absolute humidity of air at dryer exit and Wdi is the absolute humidity of air at dryer inlet.

To determine the kinetics of drying chili, drying model were used.

TABLE I. DRYING MODELS.

SN	MODEL NAME	MODEL
1	NEWTON	MR = EXP (-kt)
2	PAGE	$MR = EXP(-kt^n)$
3	HENDERSON& PABIS	$MR = a\ EXP(-kt^n)$

Initial moisture content of red chili can be determined by drying in air oven at a temperature of 105°C, till to attain constant weight. Initial moisture content was found 79.1% in the red red chili. The coefficient of determination (R2), mean bias error (MBE) and root mean square error (RMSE) are obtained from the drying model equation and used to compare the relative goodness of fit of experimental data. The highest value of R2 and the lowest values of MBE and RMSE are selected to estimate the drying curve is the best [23].

$$MBE = \frac{1}{N}\sum_{i=1}^{N}(MRpre,i - MRexp,i)^2 \quad (50)$$

$$RMSE = [\frac{1}{N}\sum_{i=1}^{N}(MRpre,i - MRexp,i)^2]^{\frac{1}{2}} \quad (51)$$

V. RESULT & DISCUSSION

The performance of the proposed multi pass solar crop dryer with reversed absorber was studied and compared with the performance of a single glazing with and without reversed absorber and multi pass solar crop dryer.

From the Fig.2 it is observed that collector efficiency (ηc) values of 35.68% and 29.80% for the MPRASCD and MPSCD respectively (when Iavg. = 674.4 w / m², Ta.avg. =34.1°C and ma = 0.0269 kg/s) and (ηc) values of 19.0% and 26.11% for the SGSCD and SGRASCD respectively. It shows that the solar air heater with reversed absorber was more efficient than conventional solar crop dryer. This observation is reliable with the other studies that the heat gain by absorber plate –II is significant [24, 25].

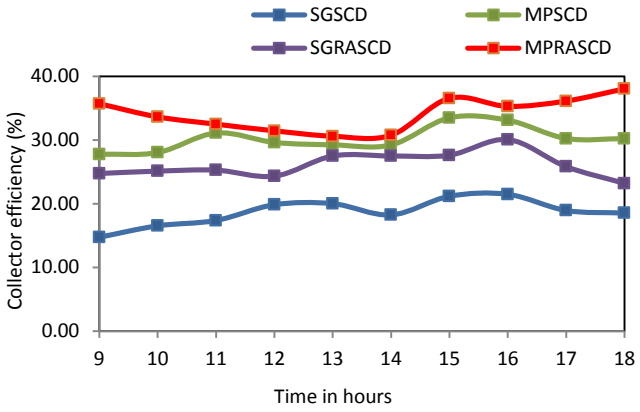

Figure 2. Variation of collector efficiency with time of the day in hour

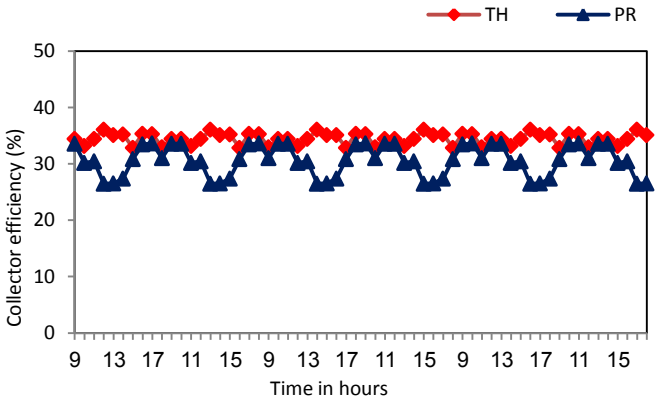

Figure 4. Plot of comparative analysis between experimental and theoretical collector efficiency for MPRASCD (Thermal model)

The energy balance Equation (1)-(7) on different components of solar drying system was solved using Excel software to find out the temperature of the air in stream-I(Tf1), stream-2(Tf2), stream-3(Tf3), temperature of absorber plate –I(Tp1), temperature of absorber plate –I(Tp2), temperature of glass–I(Tg1) and temperature of glass–2(Tg2). The results were obtained for the solar intensity and ambient air temperature of the month of March for the climatic condition of Nagpur. Fig.3 shows the hourly temperatures of the air in different streams, absorber plates and glass covers. Hourly average solar intensity and ambient air temperature was used in solving the model.

It can be observed from the air temperature curves presented in Fig.3 that the systems investigated can be used to dry a variety of agricultural products. Since the temperature of absorber plate-2 was observed higher than absorber plate –1 during the period of drying for multi pass solar crop dryer with reversed absorber [12].

From the Fig.4 it can be observed that most of experimentally attained efficiency is lesser than the theoretical efficiency obtained from the thermal analysis. Average collector efficiency obtained from the formulation and experimental for MPRASCD is 35.5% and 34.04% respectively.

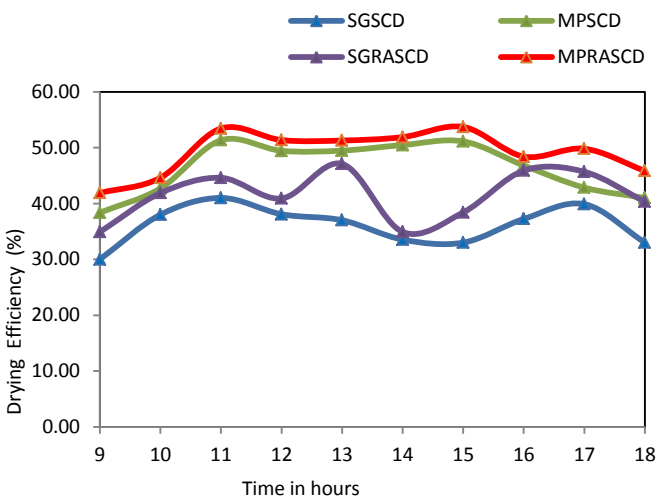

Figure 5. Variation of dryer thermal efficiency with time of the day in hour

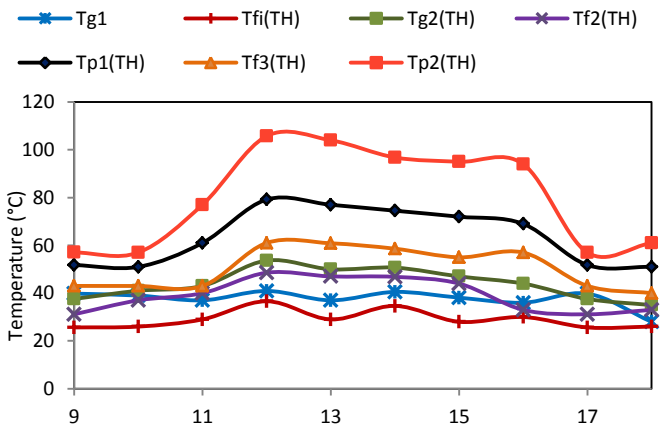

Figure 3. Hourly variation in temperature of different component of multi pass solar crop dryer with reversed absorber.

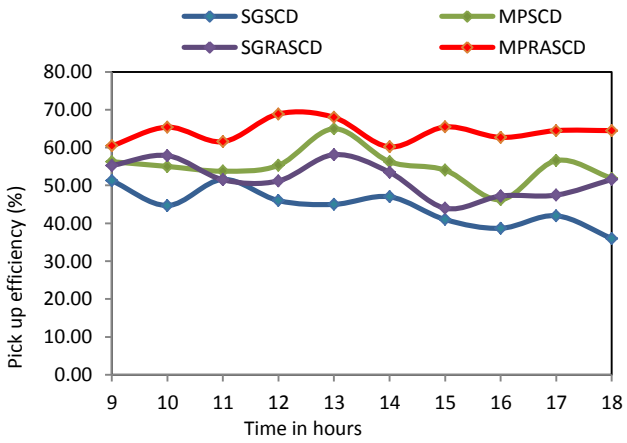

Figure 6. Variation of pick-up efficiency with time of the day in hour

From the Fig. 5 & 6 it is observed that dryer thermal efficiency (ηd) values of 49.22% and 46.35% and pick-up efficiency (ηp) value of 64.16% and 55.04% for the MPRASCD and MPSCD respectively (at Iavg.=674.4w/m², Ta.avg.=34.1°C and ma=0.0269kg/s). Dryer thermal efficiency (ηd) values of 47.86% and 37.17% and pick-up efficiency (ηp) value of 54.71% and 45% for the SGRASCD and SGSCD respectively (at Iavg.=648 w/m², Ta.avg.=30 °C and ma=0.0269kg/s). It seems that the Multi pass solar crop dryer with reversed absorber is more efficient

Fig.7 shows the profile of the moisture content versus drying time. From this plot, the moisture content in red chili above the equilibrium moisture content in MPRASCD is for shorter time than solar dryer without reversed absorber. It also observed that the moisture content in red chili is for shorter time as compared to SGRASCD. Fig.8 shows the profile of the drying rate versus drying time. Drying rate was found higher in multi pass solar crop dryer with reversed absorber than solar dryer without reversed absorber plate because of high drying temperature which reduced the effect of variation in relative humidity during sunshine hours [26].

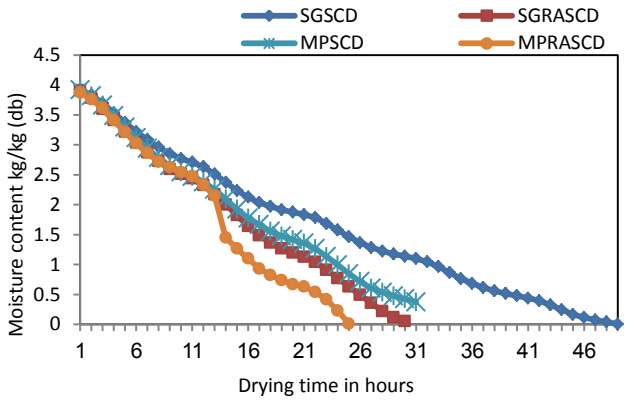

Figure 7. Hourly variation of moisture content, (db) with drying time

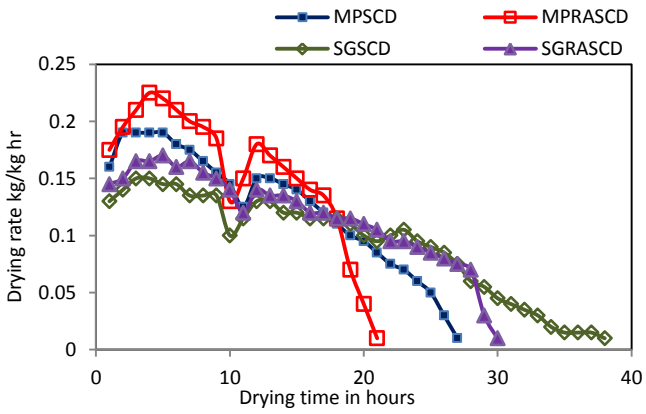

Figure 8. Hourly variations in drying rate with drying time

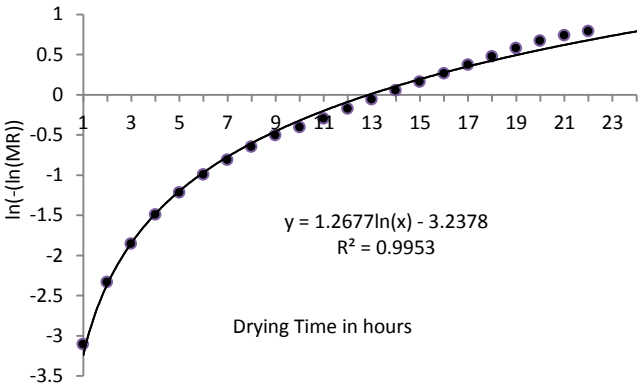

Figure 9. Plot of ln (-ln MR) versus drying time (Page's model) for MPRASCD

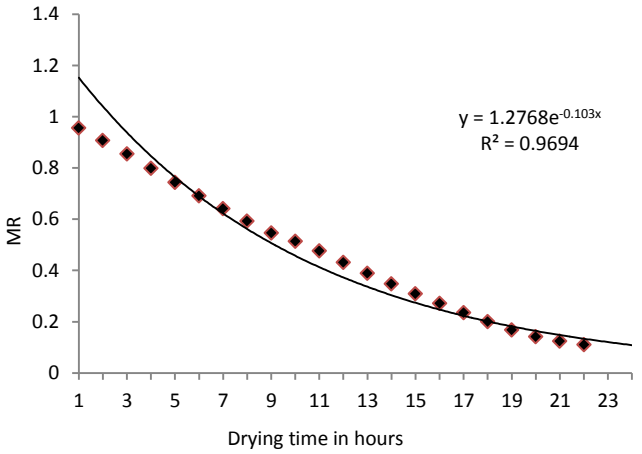

Figure 10. Plot of Moisture ratio versus drying time (Newton's model) for MPRASCD.

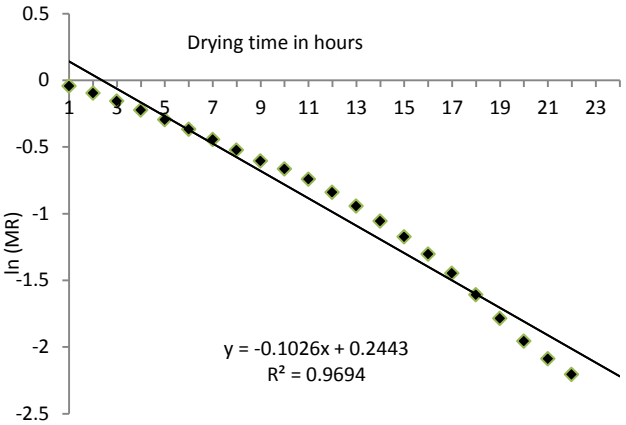

Figure 11. Plot of ln (MR) versus drying time (Henderson's and Pabis model) for MPRASCD

Fitting some of the drying model has been done with the experimental data of drying chili. Drying models such as Page model, Newton model and Henderson and Pabis model was fitted with the experimental data of drying chili. Drying experimental data in the form of changes in moisture content vs. drying time was fitted in the model of drying. In this drying models, changes in moisture content versus time calculated using Excel, and constants calculated by graphical method. Fig.9 to Fig.11 shows the results fitted the drying models with experimental data of drying. Highest value of R2 and the lowest value of MBE and RMSE were selected to estimate the best drying curve [27]. Page model can also be written in the form,

$$\ln(-lnMR) = \ln(k) + nln(t) \quad (52)$$

Equation 10 shows the relationship in ln (-ln MR) versus t, is the curve of the logarithmic equation, as shown in Fig. 9.

Henderson and Pabis equation can also be written as

$$\ln MR = -kt + \ln a \quad (53)$$

From equation 11, a plot of ln(MR) vs. drying time is a straight line with slope = k, and intercept = ln a. Graph ln (MR) vs. t, is shown in the Fig. 11.

TABLE II. CONSTANTS VALUE FITTING OF NEWTON MODEL

Dryer type	Drying model	Model constant	MBE	RMSE	R^2
MPSCD	Newton	k=0.07	0.0019	0.044	0.97
MPRASCD	Newton	k=0.1	0.0058	0.243	0.96

TABLE III. CONSTANTS VALUE FITTING OF PAGE MODEL

Dryer type	Drying model	Model constants	MBE	RMSE	R^2
MPSCD	Page	k=0.036	0.0001	0.009	0.99
		n=1.186			
MPRASCD	Page	K=0.039	0.004	0.021	0.99
		n =1.267			

TABLE IV. CONSTANTS VALUE FITTING OF HENDERSON AND PABIS MODEL

Dryer type	Drying model	Model constants	MBE	RMSE	R^2
MPSCD	Henderson & PabisS	a=1.16	0.0010	0.033	0.98
		k=0.077			
MPRASCD	Henderson & Pabis	a=1.276	0.0037	0.062	0.969
		k=0.102			

Results are given in Table 2 to Table 4 shows the Page's drying model has the highest value of R2, as well as the values of MBE and RMSE is the lowest compared to Newton and Henderson and Pabis model, so Page's model is the suitable model for Chili drying.

VI. CONCLUSION

The efficiency of a multi pass solar air collector with reversed absorber and effect of solar radiation on collector efficiency was studied. A theoretical efficiency compared with experimentally determined values with an average standard error estimation of 8.8%. Temperature of air flow was obtained from energy balance equations by solving the simultaneous equations formed for each elements of a multi pass solar air collector. Excel software with matrix inversion method was used to solve simultaneous equations. The theoretical and experimental efficiency of a multi pass solar air collector with reversed absorber can be obtained for a given sets of operating conditions.

There is a significant increase in the collector efficiency, dryer efficiency and pick-up efficiency of the solar crop dryer using reversed absorber plate. Further, results showed that for the air mass flow rate the collector temperature difference increase with increasing solar radiation (I), and decreases as solar radiation drops to lower values later on during the day. The maximum collector efficiency obtained is 38.02% and 33.48% for both multi pass with reversed absorber solar air heaters and conventional solar air heater respectively at air mass flow rate of 0.0269 kg/s.

This paper also presents the mathematical modeling of dried Chili. Three drying models have been used in order to illustrate the best drying model for Chili at constant mass flow rate. The best drying model was decided through the values of R2, MBE and RMSE. Based on the drying model curves, it has been found that Page's model is the best drying model to describe the drying curves of red chili. It is clearly showed that the experimental data was fit to the Page's model than Newton's and Henderson & Pabis model. The Page's model was resulted in the highest value of R2 and lowest values of MBE and RMSE.

NOMENCLATURE

A area, m2
L length of dryer and absorber plate-I, m
W breadth of dryer and absorber plate-I, m
C specific heat at constant pressure, J/ kg K
h height, m
hc convective heat transfer coefficient, w/ m²K
hr radiative heat transfer coefficient, w/ m²K
hw convective heat transfer coefficient due to wind, w/m²K
Ieff effective solar radiation on absorber plate-II, w/m²
I solar radiation on inclined absorber plate, w/ m²
K thermal conductivity, W/ m K
Nu Nusselt number
R universal gas constant, J /K mol
Re Reynolds number
Pr Prandtl number
T temperature, K
ΔT temperature difference, K

t time, s
U overall heat loss coefficient from sides of dryer, w/m²K
vw wind velocity, m/ s
va velocity of air, m/ s
α absorptivity
ε emissivity
ρ′ reflectivity of reflector
ρ density, kg/ m³
σ Stefan–Boltzmann constant, W/ m² K
τ transmitivity

SUBSCRIPTS

a ambient air
f1 air stream-I
f2 air stream-II
f3 air stream-III
g glass cover
g1a glass cover-I to ambient air
g1f1 glass cover-I to air stream - I
g2f2 glass cover to air stream-II
gsky glass cover to sky
p1 absorber plate-I
p1f2 absorber plate-I to air stream-II
p2 absorber plate-II
p1f3 absorber plate-I to air stream-II
p2f3 absorber plate-II to air stream-II
p1g2 absorber plate-I to glass cover -II

REFERANCES

[1] A. Fudholi, K. Sopian, M. H. Ruslan, M.A. Alghoul, and M. Y. Sulaiman. Review of solar dryers for agricultural and marine products, *Renewable & Sustainable Energy Review*,2010,vol. 14, pp. 1-30.

[2] A. Fudholi**,** M. H. Ruslan, M. Y. Othman, M. Yahya, Supranto, A. Zaharim, and K. Sopian, Collector efficiency of the double-pass solar air collector with fins in *Proc. of the 9th WSEAS Int. Conf. on SISTEM SCIENCE and SIMULATION in ENGINEERING (ICOSSSE'10),* Japan, 2010,pp. 428-434

[3] A. Fudholi**,** M. H. Ruslan, M. Y. Othman, M. Yahya, Supranto, A. Zaharim, and K. Sopian, Experimental study of the double-pass solar air collector with staggered fins, in *Proc. of the 9th WSEAS Int. Conf. on SISTEM SCIENCE and SIMULATION in ENGINEERING (ICOSSSE'10),* Japan, 2010, pp. 410-414.

[4] A. Fudholi, M. H. Ruslan, L.C. Haw, S. Mat, M. Y. Othman, A. Zaharim and K. Sopian, Performance of Finned Double-Pass Solar Air Collector, in *American Conference on Applied Mathematics (AMERICANMATH'12),* USA,2012.

[5] A. Fudholi, M. H. Ruslan, L.C. Haw, S. Mat, M. Y. Othman, A. Zaharim and K. SopianCost Analysis of Double-Pass Solar Collector with Finned Absorber, in *9th WSEAS Int. Conf. on Heat and Mass Transfer (HMT'12),* USA, ,2012.

[6] A. Fudholi, M. H. Ruslan, L.C. Haw, S. Mat, M. Y. Othman, A. Zaharim and K. Sopian Mathematical Model of Double-Pass Solar Air Collector with Longitudinal Fins, in *9th WSEAS Int. Conf. on Heat and Mass Transfer (HMT'12),* USA, Latest Trends in Renewable Energy and Environmental Informatics ISBN: 2012,978-1-61804-175-3-282, ,

[7] A. Fudholi, K. Sopian, M. H. Ruslan, M. Y. Othman, and M. Yahya,M. Thermal efficiency of double pass solar collector with longitudinal fins Absorbers, *American Journal of Applied Sciences*, 2011,vol. 8, no. 3, pp. 254-260,

[8] A. Fudholi, K. Sopian, M. Y. Othman, M. H. Ruslan, M. A. Ghoul, A. Zaharim A and Zulkifly, Heat transfer correlation for the vgroove solar collector, in *Proc. of the 8th WSEAS Int. Conf. on SIMULATION, MODELING and optimization (SMO'08)*, Spain, 2008, pp. 177-182.

[9] K. Sopian, Supranto, W. R. W. Daud, B. Yatim, and M. Y. Othman, Thermal performance of the double-pass solar collector with and without porous media, *Renewable Energy*, 1999, vol.18, no. 4, pp.557-564.

[10] R. K. Goyal and G. N. Tiwari, Parametric study of a reverse flat plate absorber cabinet dryer: A new concept, Solar Energy: 1997, 60(1) 41-48.

[11] Jain D, Jain R. K., Performance evaluation of an inclined multi-pass solar air heater with in-built thermal storage on deep-bed drying application, J Food Eng; 2004,65:497–509.

[12] Jain D. Modeling the performance of the reversed absorber with packed bed thermal storage natural convection solar crop dryer, J Food Eng; 2007,78: 637–47.

[13] A. Fudholi, K. Sopian, M. H. Ruslan, M. Y. Othman, and M. YahyaAnalytical and experimental studies on the thermal efficiency of the double-pass solar collector with finned absorber, *American Journal of Applied Sciences*, 2011, vol. 8, no. 7, pp. 716-723

[14] Lui. B. Y. H. , & Jordan R. C. Daily insolution on surfaces tilted towards equator, ASHRAE Journal. 1962,3(10). 53.

[15] K.S. Ong, Thermal performance of solar air heaters: mathematical model and solution procedure, Solar Energy, 1995, 55(2):93-109

[16] P. Naphon, On the performance and entropy generation of the double-pass solar air heater with longitudinal fins, Renewable Energy, 2005, 30:1345-1357.

[17] A. Basria, A. Yousef, N.M. Adam, K. Sopian, A. Zaharim, M.A. AlGoul, Analysis of single and double passes v-groove solar collector with and without porous media, International Journal of Energy and Environment, 2007, 2(1):109-114.

[18] K. Sacilik, Effect of drying methods on thin-layer drying characteristics of hull-less seed pumpkin, Journal of Food Engineering, 2007, 79 (1) 23-30.

[19] I. T. Togrul and D. Pehlivan, Modelling of thin layer drying kinetics of some fruits under open-air sun drying process, Journal of Food Engineering, 2004, 65 413-425.

[20] A. Midilli, H. Kucuk and Z. Yapar, A new model for single layer drying, Drying Technology, 2002, 20 (7) 1503-1513.

[21] O. Yaldız, C. Ertekin and H. I. Uzun, Mathematical modelling of thin layer solar drying of sultana grapes, Energy-An International Journal, 2001, 26 457-465.

[22] I. Doymaz, Sun drying of figs: an experimental study, Journal of Food Engineering, 2005, 71 (4) 403-407.

[23] E. K. Akpinar, Y. Bicer and A. Midilli, Modeling and experimental study on drying of apple slices in a convective cyclone dryer, Journal of Food Process Engineering, 2003, 26 (6) 515-541.

[24] H. O. Menges and C. Ertekin, Thin layer drying model for treated and untreated stanley plums, Energy Conversion and Management, 2006, 47 (15-16) 2337-2348.

[25] T. Günhan, V. Demir, E. Hancioglu and A. Hepbasli, Mathematical modelling of drying of bay leaves, Energy Conversion and Management, 2005, 46 (11-12) 1667-1679.

[26] A. Midilli and H. Kucuk, Mathematical modeling of thin layer drying of pistachio by using solar energy, Energy Conversion and Management, 2003, 44, 1111-1122.

[27] V. Shanmugam and E. Natarajan, Experimental study of regenerative desiccant integrated solar dryer with and without reflective mirror, Applied Thermal Engineering 2007, 27, 1543–1551.

[28] J. Mimba, Design and development of a solar grain dryer incorporating photovoltaic powered air circulation, Energy conservation and Management 1996, 37, 615-625.

[29] Kamil Sacilik, Rahmi Keskin, Ahmet Konuralp Elicin, Mathematical modelling of solar tunnel drying of thin layer organic tomato, Journal of Food Engineering 2006, 73 231–238.

[30] C. L. Weller, J. M. BunnDrying rate constants for yellow dent corn as affected by fatty acid ester treatment, American Society of Agriculture Engineering , 1993, 36 815-819.

[31] M. A. Leon, S. Kumar, S. C. Bhattacharya, A comprehensive procedure for performance evaluation of solar food dryer, Renewable and sustainable Energy Reviews 6, 2002, 367-393.

[32] A. A. El-Sebaii, S. Aboul-Enein, M.R.I. Ramadan, H. G. El-Gohary, Emperical correlation for drying kinetics of some fruits and vegetables, Energy 27, 2002, 85-859.

[33] M.A. Hossain and B.K. Bala, (2007) Drying of hot chilli using solar tunnel drier, Solar Energy 81, 85–92

[34] Ibrahim, M., K. Sopian and W.R.W. Daud., Study of the drying kinetics of lemon grass, American Journal 0f Applied Sciences 6 (6): 2009,1070-1075.